Received November 26, 2020, accepted December 4, 2020, date of publication December 14, 2020,
date of current version January 4, 2021.

Digital Object Identifier 10.1109/ACCESS.2020.3044419

Typhoon Inversion Method Combined With the YanMeng Wind Field and a Meteorological Monitoring System for Transmission Lines

LIQIANG AN[1], YONGYU GUAN[1], ZHIJIAN ZHU[1], JINGLI LIU[2], AND ZHUOBO NIU[2]
[1]Department of Mechanical Engineering, North China Electric Power University, Baoding 071003, China
[2]State Grid Hebei Electric Power Company Ltd., Baoding Power Supply Branch Company, Baoding 071000, China

Corresponding author: Liqiang An (anliqiang@ncepu.edu.cn)

This work was supported in part by the National Natural Science Foundation of China under Grant 51675179, and in part by the Science and Technology Project of State Grid Corporation of China under Grant SGHEBD00FCJS2000217.

ABSTRACT Extreme weather like typhoon leaves significantly terrible influence on the stability of power grid in the coastal area. A high-voltage transmission line includes hundreds of towers and usually stretches hundreds of kilometers. It is not economical to install typhoon monitoring system throughout the transmission line. This paper proposes a typhoon inversion method (TIM) for transmission line which utilizes engineering wind field model and only requires monitoring data from a few towers. The developed method is called YanMeng wind field (YM) with directional mutation genetic algorithm (DMGA) for transmission lines, or YM-DMGA method. DMGA utilizes real-time monitoring data, and improves simulation accuracy of average wind speed by dynamically optimizing two critical parameters B and z_0 in wind field model, which is a great improvement over the traditional YM model relying on historical data. The TIM is mainly composed of three parts, the meteorological monitoring system (MMS), the YM-DMGA model, and the software system. The TIM collects real-time measured wind data of particular monitoring stations through the MMS. Meanwhile, wind data of the whole transmission line is simulated using the YM-DMGA and displayed by the software system. Then the method proposed is verified to be effective in three aspects. First of all, the YM-DMGA method has great enhancement in accuracy, for the coefficient of determination R_{square} increases from 0.811 to 0.986. Secondly, DMGA in the method has quicker convergent speed than typical GA, with fitness converged in the 269th epoch, earlier than that for typical GA, 656th epoch. Lastly, DMGA has better optimal fitness value of 0.6239, bigger than that of typical GA, 0.5891. At the end of the paper, an application of the method to an 110kV double-circuit transmission line is presented to reveal the risk under the impact of the super typhoon Rammasun.

INDEX TERMS Typhoon inversion method, transmission lines, meteorological monitoring system, wind field, genetic algorithm.

NOMENCLATURE

B	Holland pressure profile parameter
β	typhoon moving direction.
c	typhoon moving speed.
C_d	drag coefficient.
f_c	Coriolis force parameter.
$\boldsymbol{F_t}$	boundary layer friction force.
F	fitness of an individual.
F_x	fitness value of individual x.
H_g	height of gradient wind speed.
H	height from the ground.
h	mean roughness length.
$\boldsymbol{k}$	a unit vector.
n	population size.
ρ_a	air density.
P_0	air pressure of the typhoon center.
P_x	probability of selection for individual.
r	radius distance from the simulated point to the typhoon center.
R_{max}	the maximum wind speed radius.
$\boldsymbol{v_t}$	typhoon wind speed.

The associate editor coordinating the review of this manuscript and approving it for publication was Andrei Muller.

$\boldsymbol{v_g}$	gradient wind speed.
$\boldsymbol{v_f}$	surface friction wind speed.
v	speed at the simulated point.
V_{max}	the maximum wind speed among the typhoon structure.
$v_{t,i}$	simulated average wind speed at i^{th} monitoring point.
$v_{r,i}$	real-time measured average wind speed at i^{th} monitoring point.
Z'	height in the calculation coordinate system.
Z_x	height with x meters above the mean roughness length.
z_0	equivalent roughness length.
θ	angle of simulated point in the coordinate system.
φ_{ltd}	latitude of typhoon center.
φ_{lgd}	longitude of typhoon center.
$\Psi_{t,i}$	simulated wind direction at i^{th} monitoring point.
$\theta_{r,i}$	real-time measured wind direction at i^{th} monitoring point

I. INTRODUCTION

Typhoon is a frequent natural disaster in western Pacific. Figure 1 shows typhoon road map of west Pacific in 2018, the year when 29 tropical cyclones reached the intensity of typhoon. Typhoon weather is a great threat to power grid in the coastal areas, leaving extremely harmful impact on the operation of the transmission lines like windage yaw flashovers and even tower collapses [1]. Figure 2 shows collapsed towers due to typhoon weather. An [2], [3] studied the structural failure of transmission towers impacted by the super typhoon Rammasun, pointing out that excessive wind speed and dynamic effect of wind/rain loads are the root cause for tower collapse. He [2] built up the finite element model of a transmission line section to analyze the relation between wind speed magnitude/direction and the maximum stress of tower members. The stability limit of transmission line was also evaluated in his research. The results showed that dynamic load leaves inevitable effect on the dynamic response of tower-line system. Literature [3] proposed a meteorological monitoring system for transmission line that can be used to assess the risk of tower collapse under typhoon weather. Fu *et al.* [4], [5] pointed out that accompanying rainwater under typhoon weather affects the aerodynamic damping properties of conductor and increases the load acting on tower-line system.

At present, there are roughly two ways to obtain the wind speed of transmission line within the influence of typhoon, one of which is meteorological monitoring. Ma [7] developed a novel anemometer to measure wind speed for overhead transmission line monitoring on the basis of the fiber Bragg grating (FBG) sensing technique. Geng [8] proposed early warning method of overhead transmission line to predict the damage probability of overhead transmission line based on geographic information and meteorological information.

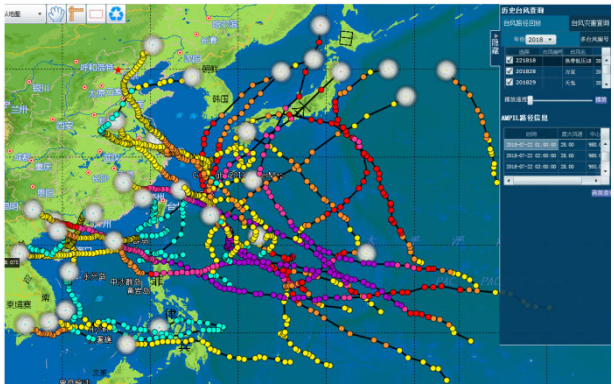

FIGURE 1. Western Pacific typhoon road map in 2018 [6].

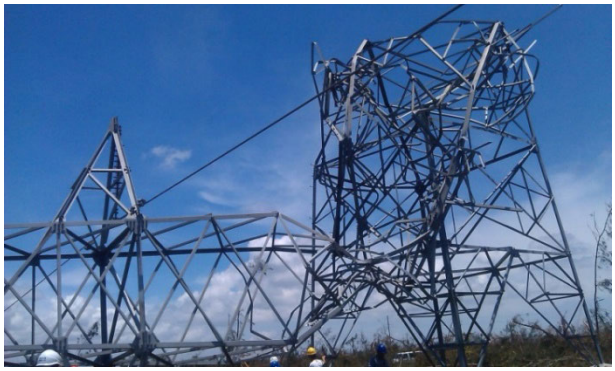

FIGURE 2. Collapsed transmission line in Hainan Island due to the Rammasun in 2014.

Typhoon data can be monitored through meteorological satellite [9], radar [10], microwave radiometric observation [11] *et al.* These observation methods are designed for meteorological researches, and focused on the macro characteristics of typhoon. Therefore it's hard to apply them on evaluating the transmission towers' wind resistance performance.

The other approach is numerical simulation based on typhoon wind field model. Meteorological wind field model is used for weather forecasting. Based on fluid mechanics and thermodynamics theory, the meteorological typhoon model considers a complex physical formation process and mainly simulates some basic features of typhoon. However, meteorological wind field model usually has a complicated structure and a large amount of calculation, which brings great inconvenience. Therefore, scholars and researchers have put in numerous efforts to establish engineering typhoon models and have been working on enhancing accuracy and calculation efficiency of typhoon models [12]. There are several engineering typhoon model and each has its own theories and characteristics. Thompson *et al.* adjusted the thickness of the boundary layer and improved the drag coefficient to make the CE wind field closer to the actual typhoon structure [13]. Although its accuracy is reliable, the slow calculation can not be ignored. The Georgiou model uses the Monte Carlo simulation method for wind field research [14]. Actual data

FIGURE 3. Collapsed tower in Guangdong due to the typhoon Tiange in 2017.

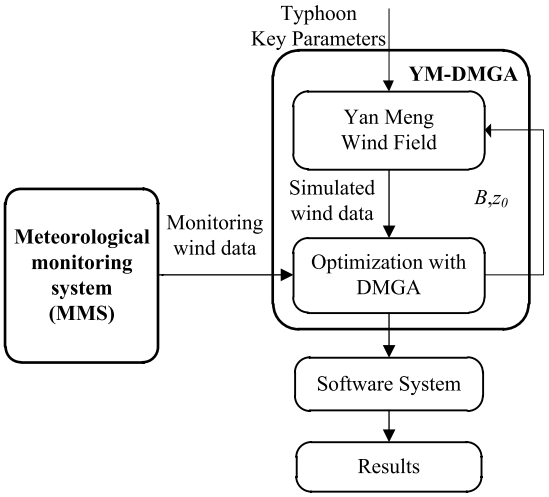

FIGURE 4. Procedure of TIM.

was used to verify wind field in this study for the first time. However, the Georgiou model ignores the influence of drag coefficient on wind speed. With strict structure theory and advanced calculation technology, the Shapiro model can effectively solve the wind speed distribution of typhoon [15]. But the value of the drag coefficient in the Shapiro model will be too high, because Shapiro uses the average wind speed in the boundary layer when calculating the drag coefficient. The YanMeng wind field model considers the boundary layer friction effect and well expresses the relationship between the forces in the typhoon wind field, suitable for engineering application [16], [17]. An [2], [3] studied the structural failure of two transmission lines under super typhoon Rammasun that occurred in mid-July 2014, using YanMeng wind field to simulate typhoon characteristics such as wind speed and direction.

Currently, due to the extraordinary length of transmission lines (a typical 110kV transmission line can stretch over 100km), meteorological monitoring cannot well reflect the wind speed of every single tower of the whole line with limited monitoring points, while the engineering wind fields need enhancement in accuracy. Therefore, this paper proposes a typhoon inversion method (TIM) named YM-DMGA with the YanMeng wind field (YM) and directional mutation genetic algorithm (DMGA) combined. The YM-DMGA method dynamically optimizes critical parameters of the wind field model, significantly improving the simulation accuracy.

The following part of the paper including several sections will explain the typhoon inversion method (TIM). Section II will show in details the structure of TIM and how it functions combining YanMeng wind field (YM) and directional mutation genetic algorithm (DMGA). Meanwhile, validation of the proposed method will be conducted in section II. Then section III will present an application of the method to an 110kV double-circuit transmission line impacted by the super typhoon Rammasun. The maximum transverse wind speed and corresponding wind attack angle of each line section were presented to reveal the risk to transmission line. At last, some conclusions about the method proposed and the prospects for the future of this field will be given in section IV.

II. PROPOSED TYPHOON INVERSION METHOD (TIM)

A. PROCEDURE

TIM for transmission lines acquires the wind speed and direction of every tower in the transmission line based on the typhoon key parameters (longitude, latitude, moving speed and moving direction of the typhoon center, central air pressure, maximum wind speed and maximum wind speed radius) and the real-time monitoring wind data. As figure 4 shows, the basic procedure of the TIM consists of three main parts, the MMS, the YM-DMGA model, and the software system.

Firstly, the MMS obtains the real-time monitoring average wind speed magnitude / direction at the particular monitoring points. Meanwhile, the YanMeng wind field simulates the average wind speed according to typhoon key parameters. Then DMGA improves the simulation accuracy of average wind through dynamically optimizing two critical parameters B and z_0 in YanMeng wind field, till the result meets accuracy condition. Finally, the 10-min average wind speed magnitude/direction of each tower among the whole transmission line at 10m height is displayed in the software system.

B. METEOROLOGICAL MONITORING SYSTEM (MMS)

1) COMPOSITION OF THE MMS

The real-time measured average wind speed of towers is obtained by the MMS. The MMS consists of five main parts as shown in figure 5: a) monitoring terminal, b) monitoring base station, c) power supply module, d) data transmission module and e) monitoring center server.

The monitoring terminal is an integrated meteorological sensor, model EWM-50, which can measure the temperature, wind speed, wind direction, air pressure and rainfall simultaneously. The EWM-50 has the advantages of small size and impact structure. Since it uses an ultrasonic anemometer to measure the wind speed and wind direction, it has no moving

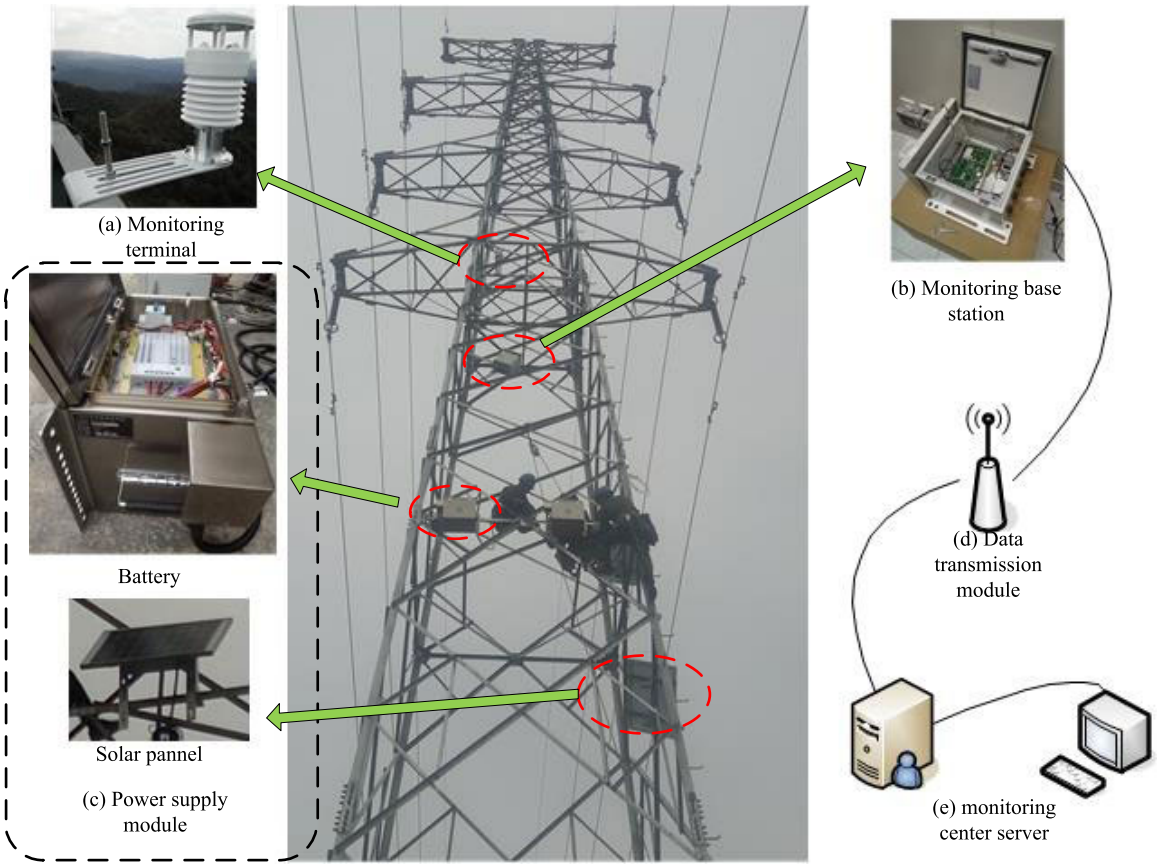

FIGURE 5. The structure of MMS.

parts and is maintenance-free. It's usually mounted on a cross member of the tower to obtain real-time measured wind data.

The power supply module is composed of a solar panel, a charge and discharge controller and a battery. A 100W solar panel charges the device, and a 150Ah gel battery is adopted to keep the system operating normally for 30 consecutive raining days. Besides, the system adopts Phocos CML series photovoltaic controller, which automatically controls the power output of solar panel and battery according to the demand of the load, and regulates the charging and discharging of the battery.

The function of the monitoring base station is to connect the monitoring terminal to the monitoring center server. The monitoring base station can process the commands received from the monitoring center server and sent them to the monitoring terminal. Then the data transmitted from the monitoring terminal can be stored centrally and sent to the monitoring center server. The monitoring base station is packaged in a metal box as shown in figure 5(b), and it has been proved by experiments that this device is rainproof, dustproof, capable to work in the temperature range from −40 °C to 70 °C, and has functions such as lightning protection, anti-electromagnetic interference, etc. In case of a malfunction, the monitoring base station can restart automatically. Moreover, it can execute a scheduled restart or a restart command from monitoring center. Figure 5 shows the installation of the monitoring base station. All the monitoring data, including average wind speed and wind direction are sent to the monitoring center server for further utilization in the following.

The technical parameters of the MMS are shown in table 1.

TABLE 1. Techinical parameters of mms.

Working environment	temperature：-40 °C～ 60°C humidity：0 ～ 100%RH
Monitoring terminal	temperature：-40°C～+80°C；±0.2°C wind speed：0～75m/s；±0.3m/s wind direction：0～360°；±3° air pressure：500hPa～1100hPa；±1hPa rainfall：0～999.9mm/day；±0.4mm
Power supply module	Powered by solar and high performance polymer battery solar cell 100W battery 150Ah Power supply: solar and battery powered; Protection level: IP65;
Monitoring Base station	Should be satisfied to work in the absence of sunlight for 30 days; Battery life: ≥12 years; Solar battery life: ≥12 years.

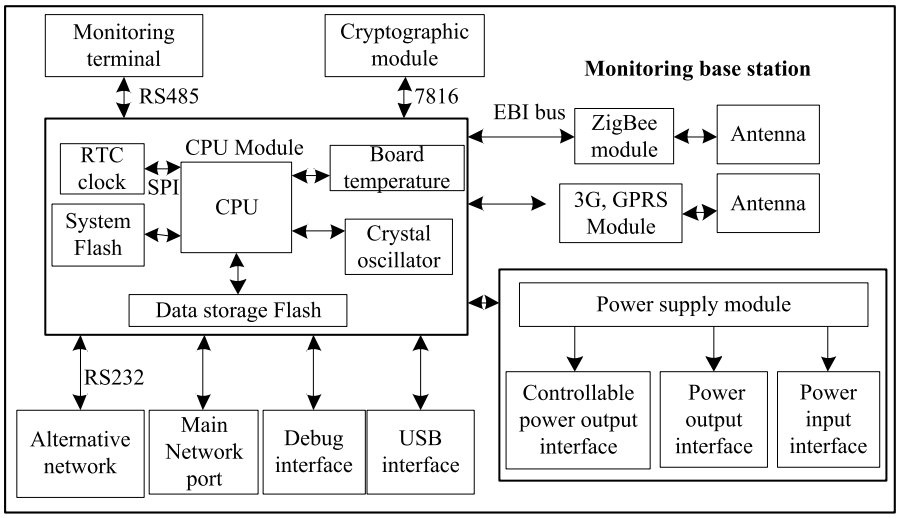

FIGURE 6. The structure of monitoring base station.

2) HARDWARE DESIGN OF MONITORING BASE STATION

The monitoring base station mainly consists of three printed circuit boards (PCBs), a motherboard, a Zigbee wireless interface board, and an encrypted interface board, as shown in figure 6. The system uses wireless or wired access, and can also be accessed through an Ethernet external module, such as an optical fiber or WIFI expansion system.

The CPU module includes a CPU, a system flash, a data storage flash, a real-time clock, a board temperature sensor, a crystal oscillator, etc. The CPU module is the core part of the monitoring base station and is responsible for the scheduling of the entire system, the calculation, storage, and transmission of data. Model atc cpu-at91sam9g20 is selected according to the data processing capability, operating environment, power consumption requirements of the system design.

Zigbee module is a short-range, low-power wireless communication technology based on the IEEE802.15.4 standard, including power control, reset control, connectors, etc. The IRIS Base model is selected in this system, has communication distances from 100 meters to 1200 meters, featuring 51-pin socket connection, compact design, small size, chip-mount pad design, built-in chip or external Sub-Miniature-A (SMA) antenna. Moreover, it includes ADC, DAC, comparator, multiple IO, I2C and other interfaces to connect user's product.

Huawei 770W module is selected in 3G, GPRS general module of the system. With a GPRS module, the device is capable to realize long-distance wireless transmission of data through the existing wireless communication network. It receives commands from the monitoring center, sets the sampling frequency and other parameters, while stores the data and sends it to the monitoring center. To ensure the accuracy of time, the monitoring base station calibrates time as the monitoring center commands, the error does not exceed 5s, and the clock travel error is less than 1s within 24 hours.

C. THE YM-DMGA (YANMENG-DIRECTIONAL MUTATION GENETIC ALGORITHM)

1) THE YANMENG WIND FIELD

As can be seen in the figure 4, the YanMeng wind field model is adopted in the TIM for numerical simulation of 10-min average wind speed at 10m height. The equilibrium equations of the YanMeng typhoon wind field considering the pressure gradient of the boundary layer friction can be written as [16], [17]:

$$\frac{\partial \boldsymbol{v_t}}{\partial t} + \boldsymbol{v_t} \cdot \nabla \boldsymbol{v_t} = -\frac{1}{\rho_a} \nabla p_a - f_c \boldsymbol{k} \times \boldsymbol{v_t} + \boldsymbol{F_t} \tag{1}$$

where, $\boldsymbol{v_t}$ is the typhoon wind speed, ρ_a is the air density, f_c is the Coriolis force parameter, and $\boldsymbol{F_t}$ is the boundary layer friction force, $\boldsymbol{k}$ is a unit vector. The speed of air movement can be decomposed into the vector sum of the gradient wind speed, $\boldsymbol{v_g}$ and the surface friction wind speed $\boldsymbol{v_f}$ in the free boundary layer as equation (2) expressed.

$$\boldsymbol{v_t} = \boldsymbol{v_f} + \boldsymbol{v_g} \tag{2}$$

The coordinate systems of YanMeng wind field in horizontal and vertical direction are shown in figure 7. Where, r is the radius distance from the simulated point to the typhoon center, v is typhoon speed, c is typhoon moving speed, β is the typhoon moving direction, θ is the angle of simulated point in the coordinate system, Z' is the height in the calculation coordinate system, h is the mean roughness length related to z_0, Z_x represents x meters above the mean roughness length h, H_g is the height of gradient wind speed, H is the height from the ground.

Figure 8 demonstrates the flowchart of the YanMeng wind field model. The first step is to mesh the wind field solving domain in the polar coordinate system. The meshing in the radial direction is designed to be uneven to properly enhance the wind field solving efficiency and simulation accuracy of inner area. As can be seen in figure 7(a), the wind field near

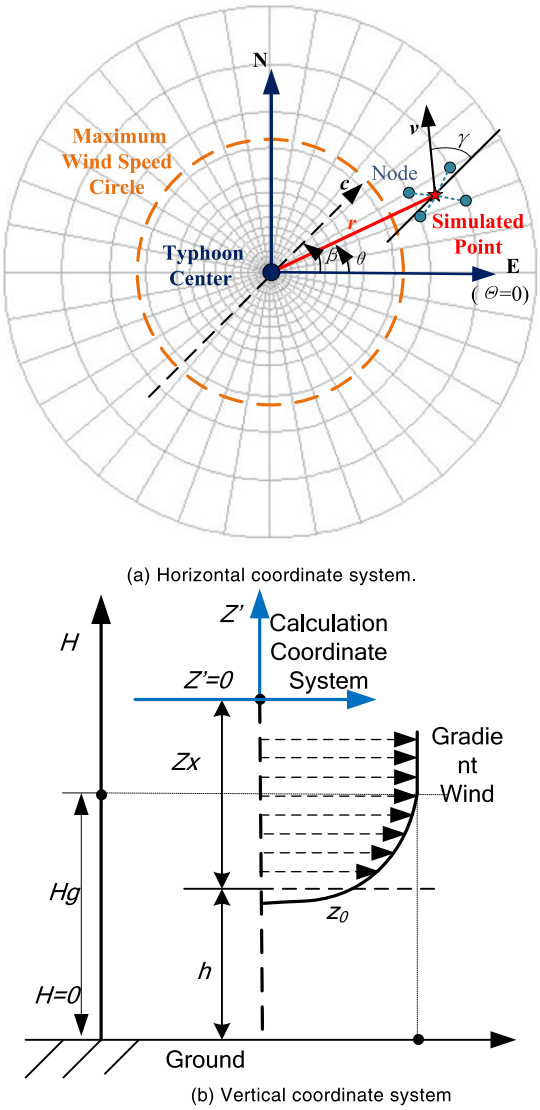

FIGURE 7. Coordinate system of YanMeng wind field.

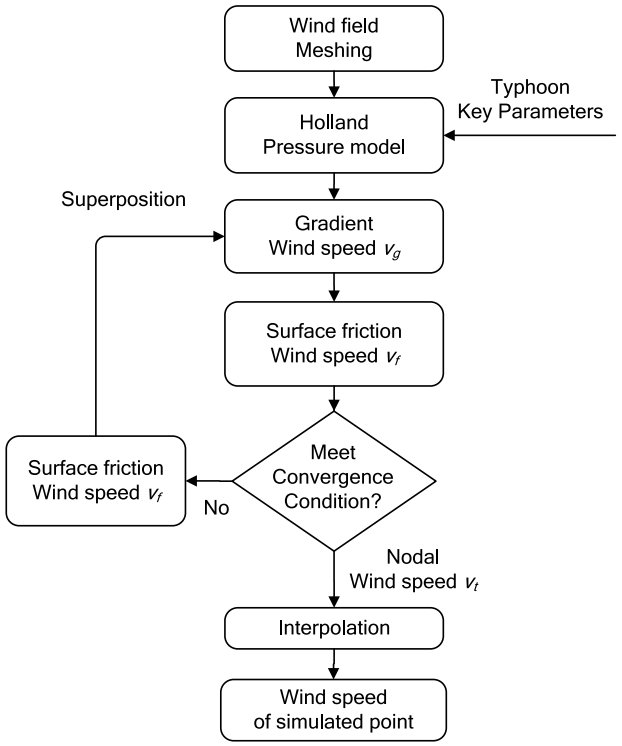

FIGURE 8. The flow chart of the YanMeng wind field.

TABLE 2. Typhoon key parameters.

Typhoon key parameter	Parameter description
V_{max}	The maximum wind speed among the typhoon structure in m/s
R_{max}	The maximum wind speed radius
P_0	Air pressure of the typhoon center in hPa
c	Typhoon moving speed in km/h
β	Typhoon moving direction in °
ϕ_{ltd}	Latitude of typhoon center in °
ϕ_{lgd}	Longitude of typhoon center in °

the wind eye is meshed intensively. And when it comes to the outer area of wind field, the meshing gets sparse. In this way, the whole wind field structure can be displayed in the software system instantly with efficient calculation.

Then the typhoon parameters provided by the meteorological station is put into the Holland pressure model to calculate the gradient wind speed $\boldsymbol{v_g}$. Table 2 shows all typhoon key parameters and corresponding explanation to them. V_{max} and P_0 are used to describe the intensity of typhoon, directly affecting the simulation wind speed at target position. R_{max} is a parameter that describes the scale of typhoon and influences wind speed distribution among typhoon structure. Parameter c, β, φ_{ltd} and φ_{lgd} are used to describe geographic information of typhoon when typhoon transits and attacks transmission line. They are mainly used to calculate the distance and angle between typhoon center and the target point, which affect the simulation of wind speed magnitude and direction.

The Holland pressure model can be described with the following equation [18]:

$$P(r) = P_0 + \Delta P \cdot \exp[-(R_{\max}/r)^B] \tag{3}$$

where: $P(r)$ is the pressure of the place $r$km from the typhoon center, P_0 is the typhoon center pressure; R_{max} is the maximum wind speed radius; B is the Holland pressure profile parameter; $p = P_\infty$-P_0, P_∞ is 1010hPa.

The surface friction wind speed $\boldsymbol{v_f}$ is calculated with the gradient wind speed $\boldsymbol{v_g}$ inputted as the initial value. The $\boldsymbol{v_f}$ will be superimposed to the $\boldsymbol{v_g}$ and renew itself until it convergences. Then comes out the nodal wind speed $\boldsymbol{v_t}$, which means the simulated wind speed of every nodes of the wind field grid. Finally the wind speed of target point is calculated through interpolation.

2) OPTIMIZATION WITH DMGA

This part will explain how the YanMeng wind field and the MMS combine in the YM-DMGA. DMGA improves the

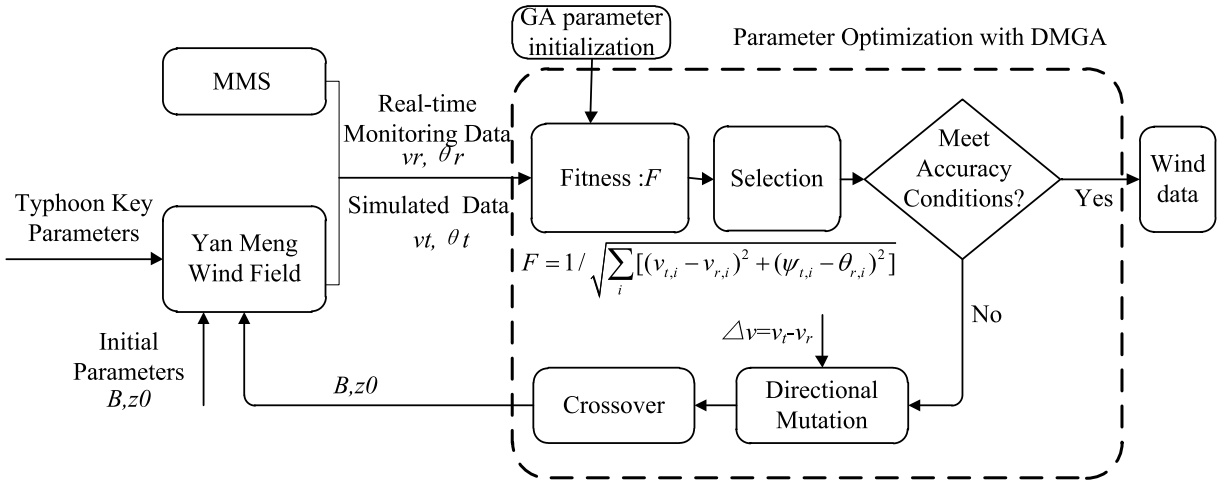

FIGURE 9. The procedure of DMGA.

simulation accuracy of average wind speed by dynamically optimizing two critical parameters, B and z_0 in the YanMeng wind field according to the real-time measured wind data and the simulated wind data.

The Holland pressure profile parameter B is a key parameter for the Holland pressure field model, which is adopted in the YanMeng wind field. As equation (3) shows, B has significant impact on the radial distribution of wind speed in the typhoon structure as well as the maximum wind speed. On the other hand, the equivalent roughness length z_0 is used to describe the friction effect due to different terrain where the target point located. The equivalent roughness length z_0 is a parameter closely related to local area situation. And theoretically one z_0 parameter is for every single tower. However, calculation frequency is required when the whole system monitors meteorological data and simulated wind speed in engineering application. Therefore, the z_0 is turned into a parameter for the whole wind field rather than a traditional one for local area. z_0 decides the drag coefficient C_d, greatly affecting the simulation accuracy.

A typical approach for determining the parameter B and z_0 so far is fitting historical meteorological data published about typhoons occurred in the region researched-. Specifically, the typical approach is to find out a parameter that minimizes the difference between the simulated wind data and the observed wind data of a certain historical time through data fitting. However, the fixed value of the two parameters determined by such way cannot reflect the time-varying characteristic of typhoon. Therefore, a new method using a genetic algorithm [19], [20] with directional mutation (DMGA) is introduced to solve this problem. In this method, comparison between simulated wind speed and real-time measured one is conducted to dynamically optimizing the two parameters. The basic procedure of DMGA is shown in figure 9.

To reduce the computation workload of DMGA, the initial parameters in the first generation are generated randomly among the approximate range of optimal solution of the two parameters, as shown in table 3, which was determined through the previously mentioned typical way, the data fitting. This is the beginning of the whole DMGA process, with corresponding parameters like probability of mutation, crossover and population size set properly.

TABLE 3. The approximate range of optimal solution of the two parameters.

parameter	B	z_0
Approximate range of optimal solution	0.8-1.05	0.01-0.15

TABLE 4. GA parameter initialization.

GA parameters	Population size	Probability of crossover	Probability of mutation
value	100	30.0%	0.5%

FIGURE 10. Coding diagram.

Three GA parameters are initialized as shown in the table 4 before the system works.

Decimal code is adopted in this system, avoiding the trouble of code conversion. An individual is encoded as shown in figure 10 with parameter B code part and parameter z_0 part.

The fitness value is used to evaluate the performance of each individual. For an individual, greater fitness valued represents more outstanding performance. In this part, the two parameters provided by each individual were put into the YanMeng wind field model, then comes out the simulated average wind speed at 10m height. It is compared with the real-time measured average wind speed recorded by the MMS to obtain the fitness value of every single individual, as expressed in the

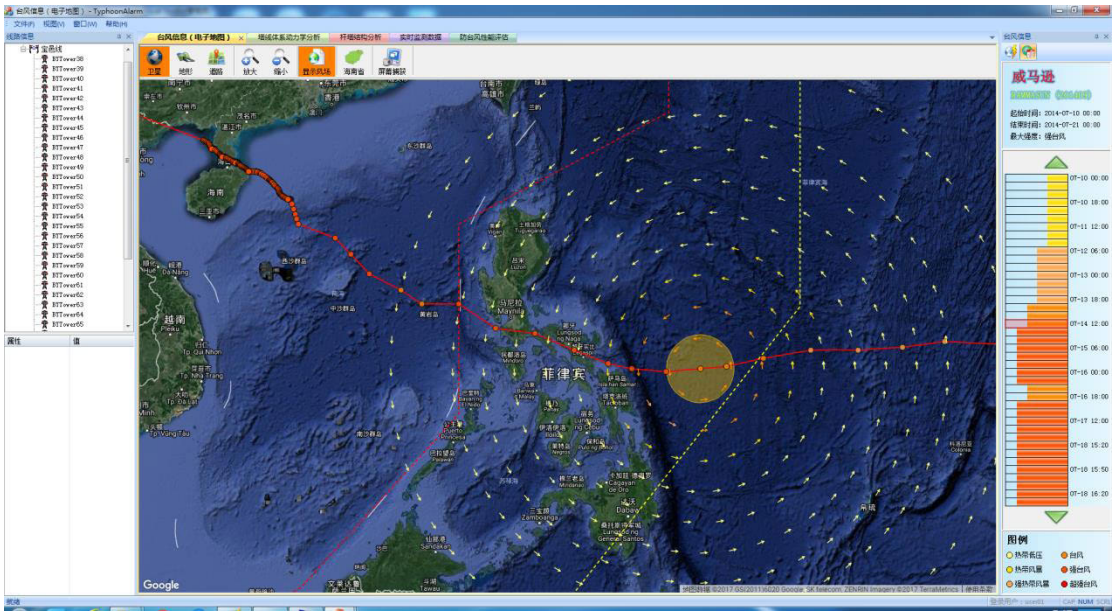

FIGURE 11. The software system.

formula (4):

$$F = 1/\sqrt{\sum_{i}[(v_{t,i} - v_{r,i})^2 + (\psi_{t,i} - \theta_{r,i})^2]} \tag{4}$$

where: F is the fitness of an individual, $v_{t,i}$ is the simulated average wind speed at i^{th} monitoring point, $v_{r,i}$ is the real-time measured average wind speed at i^{th} monitoring point, $\Psi_{t,i}$ is the simulated wind direction at i^{th} monitoring point, $\theta_{r,i}$ is the real-time measured wind direction at i^{th} monitoring point.

It's worth noting that the real-time measured data needs to be converted into 10m height wind speed from different height where sensor installed. The conversion is performed using equation (5) [21]:

$$v_0 = K_0 v_k \tag{5}$$

where, v_0 is wind speed at 10m height in m/s, K_0 is the wind speed conversion factor, v_k is wind speed at sensor's height in m/s.

Then in the selection part, those individuals with better performance will get more chances to survive, enhancing the performance of the whole generation. For every single individual, the probability of being selected for the next generation is given by the formula (6):

$$P_x = \frac{F_x}{\sum_{k=1}^{n} F_k} \tag{6}$$

where, P_x is the probability of selection for individual x, F_x is the fitness value of individual x, n is population size, the number of individuals of a generation.

The simulated wind data will be sent to the software system if meets accuracy conditions. If not, it will go to the directional mutation. Different from typical GA, the mutation is directional, enhancing the efficiency of parameter optimization. It's found in numerous tests that there is negative correlation between the simulated average wind speed and the two parameters. Therefore, the wind speed simulation error calculated is used to decide the mutation direction, as shown in figure 9. For example, if the simulation error is positive, then positive mutation will happen at random position in individual code, which will increase the two parameters' value.

D. THE SOFTWARE SYSTEM

The software system includes backstage computation module and user interface. The computation module gains data from the monitoring center server, and calculates the wind speed magnitude/direction of every grid node with YM-DMGA method. Whereas, as figure 7(a) shows, the towers are not exactly located on the grid nodes, the wind speed magnitude/direction of them is the linear interpolation of wind field data for the four nodes of the grid in which the tower is located.

The user interface is shown in figure 11, which displays the transmission line information, the typhoon center information and wind field simulation results. In addition to the title bar, menu bar and status bar, there is a workspace divided into three sections. 1) In the transmission line information display area on the left, the hierarchical structure of the lines is displayed in a tree view and the details of the lines and towers are displayed in a list. 2) On the right, typhoon center information display area consists of three parts: a tab bar showing the name of the typhoon, the start and end time and the maximum gust intensity; a detailed information column showing the meteorological information of a certain node at different times and the legend bar. 3) In the

middle, the function interfaces such as ''Electronic Map'' and ''Online Monitoring Data'' can be switched through the labels. The electric map uses the Google Map offline API, and is embedded into the application through Chromium Embedded Framework (CEF3), while the display function of the typhoon wind field is developed in JavaScript.

The interface demonstrates 10-min average wind speed magnitude/direction at 10m height simulated previously. On each wind grid node, there is an arrow, the length of which represents the wind speed while the direction represents the wind direction. In this way, the user interface gives an intuitive demonstration of the typhoon wind field, and helps better evaluate the transmission line's bearing capacity against typhoon condition.

E. VALIDATION OF THE PROPOSED METHOD

In this part, the YM-DMGA is validated through the monitoring wind data of typhoon Rammasun collected by Xuwen national meteorological station located in Guangdong, China, with geographic coordinate [110°14'52''E, 20°31'20''N]. Rammasun is a super typhoon that happened in 2014. It started from a tropical depression in western Pacific on July 9, 2014. It kept strengthening after heading into the South China Sea and became a super typhoon on July 18, 2014. It caused serious loss to power grid of southeast coastal area of China. Table 5 shows the key parameters of Rammasun from 6:00 to 24:00 on July 18, 2014 [22].

Figure 12 shows the meteorological data at a meteorological station from 14:40 to 22:30 on July 18th in 2014, when the Rammasun swept across Hainan province. The meteorological data includes the wind speed respectively simulated by typical way (data fitting) and YM-DMGA, also, the real-time wind speed. To make the comparison more quantitative, the coefficient of determination R_{square} will be used in the following analysis.

The coefficient of determination R_{square} in the figure 12 was given by the formula (7) [23]:

$$R_{suqare} = 1 - \frac{\sum_{i=1}^{m} [y_i - \hat{y}_i]^2}{\sum_{i=1}^{m} [y_i - \bar{y}_i]^2} \tag{7}$$

where: $\bar{y}$ represents the mean of real-time wind speed, $\hat{y}_i$ represents the i^{th} simulated wind speed, y_i represents the i^{th} real-time wind speed. It represents good performance of simulation when the R_{square} is close to 1.

It can be seen from figure 12 that YM-DMGA has significantly better performance in the simulation of typhoon average wind speed than that with the typical way of data fitting, as R_{square} increases to 0.986 from 0.811. The YM-DMGA proposed in this paper is proved to be significantly effective from this perspective.

Figure 13 compares the performance of DMGA and the typical GA at 2014/7/18/15:00, when the Rammasun landed Hainan province. The optimal fitness of DMGA converges in the 269$^{\text{th}}$ epoch, while that of typical GA converges in the 656$^{\text{th}}$ epoch. On the other hand, the convergent fitness value of DMGA is 0.6239, bigger than that of typical GA, 0.5891. It can be seen from figure 13 that DMGA can find the optimal fitness better and faster than typical GA.

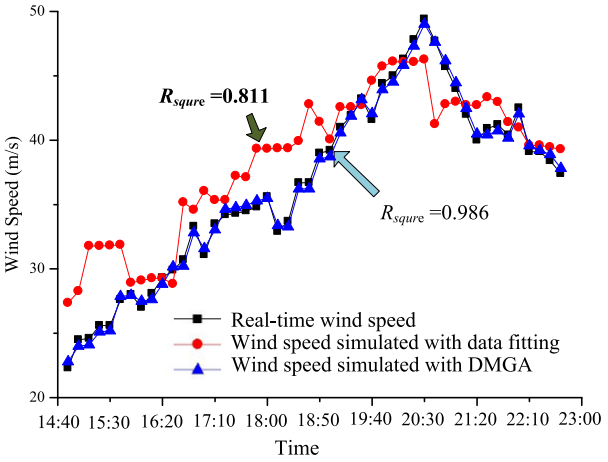

FIGURE 12. Comparison between simulation results and real-time wind speed of Rammasun.

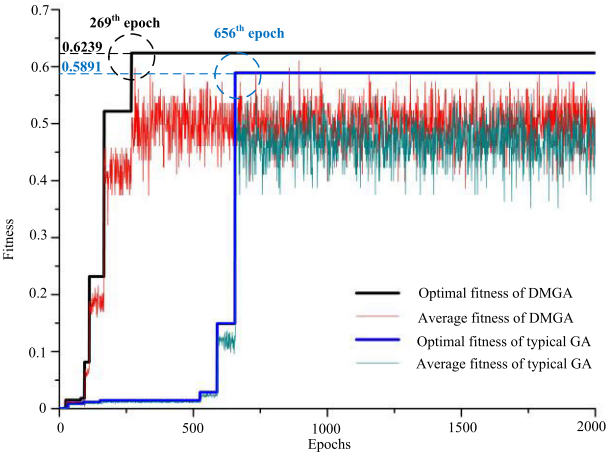

FIGURE 13. Comparison of DMGA and typical GA.

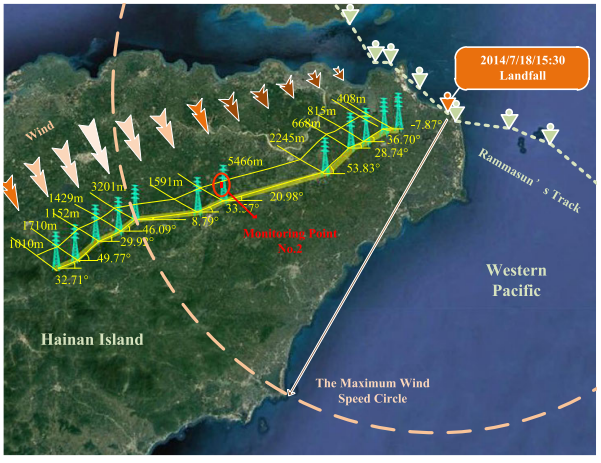

FIGURE 14. The 110kV double-circuit transmission line.

TABLE 5. Key parameter of Rammasun on July 18, 2014.

Time	Longitude	Latitude	Central Pressure (hPa)	Maximum Wind Speed Radius (km)	Moving Direction	Typhoon Center Moving Speed (m/s)
06:00	112.6	18.9	935	34.63	108.40	5.56
07:00	112.5	18.9	935	34.63	180.00	5.56
08:00	112.3	19.0	930	32.87	153.42	5.56
09:00	112.2	19.1	930	32.87	134.98	5.56
10:00	112.1	19.3	930	32.87	116.53	5.56
11:00	111.9	19.5	920	29.90	134.98	5.56
12:00	111.8	19.6	920	29.90	134.98	5.56
13:00	111.5	19.8	920	29.90	146.29	5.56
14:00	111.3	19.9	915	28.63	153.42	5.56
15:00	111	19.9	910	27.47	180.00	5.56
16:00	110.9	20.0	910	27.47	134.98	5.56
17:00	110.7	20.1	910	27.47	153.42	5.56
18:00	110.6	20.2	910	27.47	134.98	5.56
19:00	110.5	20.2	910	27.47	180.00	5.56
20:00	110.3	20.3	915	28.63	153.42	6.11
21:00	110.1	20.4	915	28.63	153.42	6.11
22:00	110	20.4	930	32.87	180.00	6.11
23:00	109.9	20.5	935	34.63	134.98	6.11
24:00	109.7	20.7	940	36.60	134.98	6.11

F. APPLICATION OF THE PROPOSED METHOD TO AN 110kV DOUBLE-CIRCUIT TRANSMISSION LINE

This section presents an application of the TIM to an 110kV double-circuit transmission line consisting of 75 towers, which suffered severely from the super typhoon Rammasun in 2014. Figure 14 shows 12 tension towers among the transmission line and other detailed information including the straight line distance between two tension towers, and the angle of each line section.

Two monitoring points in total were installed for the MMS to make sure that the monitoring data is persuasive for the transmission line with such a long length. Monitoring point No.1 and No.2 were separately installed at tower No.39 and tower No.44, which are located at the middle of the transmission line. The structure and installation of MMS are shown in figure 5.

Figure 15 shows the wind speed contour map of Rammasun at 2014/7/18/15:00, when the Rammasun landed for the first time, probably the most dangerous moment for the transmission line. Figure 15 illustrates wind speed and wind direction of nodes in a larger scale at this moment on the Google map. From figure 15, it can be seen more clearly about the radial profile of the typhoon structure. The maximum wind speed circle marked shows the most dangerous position in the typhoon wind field, where the transmission line suffered the most severe wind conditions. From this circle to the wind

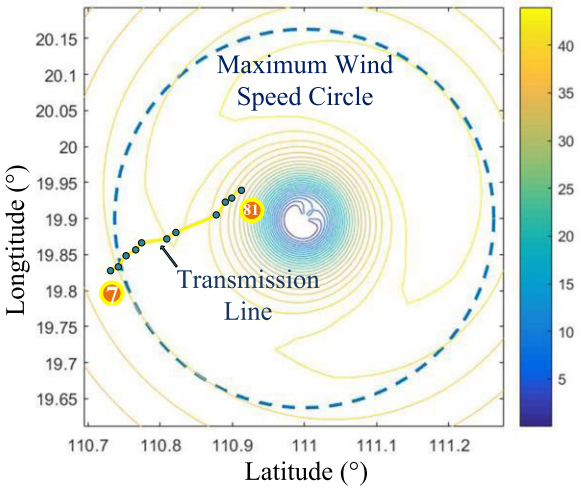

FIGURE 15. Wind speed contour map of Rammasun at 2014/7/18/15:00.

eye or to the outer area of the wind field, the average wind speed drops rapidly.

Generally speaking, it comes to the most dangerous situation when wind is perpendicular to transmission line (i.e. wind attack angle, the angle between wind and transmission line longitudinal direction, is 90 degree). Therefore the component of 10-min average wind in the transverse direction during the typhoon Rammasun swept across is calculated.

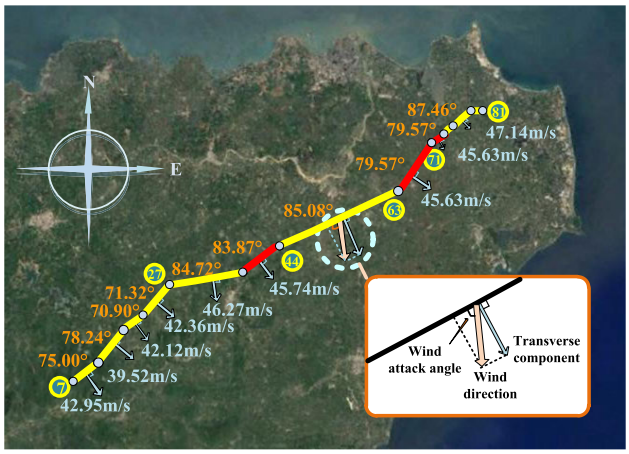

FIGURE 16. The maximum transverse wind speed of each line Section during the Rammasun.

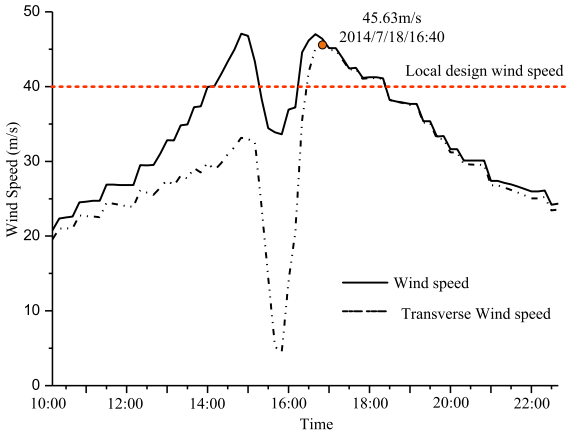

FIGURE 17. Wind speed of the collapsed tower No.66 in time history.

Figure 16 illustrates the maximum transverse wind speed and corresponding wind attack angle of each line section.

It can be inferred from figure 16 that the maximum transverse wind speed reached over 40m/s, the local design wind speed of transmission line, for most of line sections, which means great probability of tower collapse. However, whether collapse phenomenon happens not only depends on wind load applied, but also the capacity of towers, which varies a lot from one to another. The red line sections highlighted in figure 16 represents sections destroyed in this event, containing collapse towers. What is noticeable is that the collapsed towers, No.39-No.43, No.64-No.68, No.72-No.73 are all suspension tangent towers, as shown in figure 2.

Figure 17 shows the wind speed of the collapsed tower No.66 from 2014/7/18/10:00 to 2014/7/18/22:30. The solid curve represents the average wind speed while the other represents the transverse wind speed, which is taken as a critical factor that cause tower collapse. It can be inferred from figure 17 that the maximum transverse wind speed of tower No.66 is 45.63m/s, occurred at 2014/7/18/16:40, the dangerous moment for the tower No.66.

III. CONCLUSION

This paper proposes a typhoon inversion method to evaluate the transmission line's ability to resist against typhoon weather. An application of the proposed method to a 110kV double-circuit transmission line impacted by the super typhoon Rammasun is presented. Conclusions can be drawn as follow:

1)The TIM proposed in this paper mainly consists of three parts: the MMS, the YM-DMGA and the software system. The MMS collects real-time measured wind data at particular monitoring points. Meanwhile, the YanMeng wind field simulates the wind data with typhoon key parameters put in. Then DMGA enhances the simulation accuracy of typhoon average wind speed by dynamically optimizing parameters B and z_0 in the YanMeng wind field. Finally, the software system displays the typhoon inversion results.

2)The results show that average wind speed at a meteorological station simulated with YM-DMGA has better accuracy than that simulated with data fitting, with R_{square} increased to 0.986 from 0.811. Therefore it can be concluded that YM-DMGA indeed enhances the simulation accuracy of typhoon average wind speed.

3)DMGA has better performance than typical GA in the optimization process. On the one hand, DMGA has quicker convergence speed. DMGA converges in the 269th epoch, while typical GA converges in the 656th epoch. On the other hand, DMGA has better optimal fitness. The convergent fitness value of DMGA is 0.6239, bigger than that of typical GA, 0.5891.

4)The wind speed magnitude/direction of every single tower among the transmission line during typhoon weather is available through the TIM. The transverse wind speed is calculated to evaluate the danger that transmission line may encounter and to predict the moment when structural failure occurs under such extreme conditions.

5)Typhoon inversion technology will become more and more important in the field of transmission line engineering especially in coastal area. It can be used for failure analysis of tower-line system in coastal area under typhoon condition to provide some valuable suggestions for transmission line design. The concern should be place on further enhancing the accuracy and calculation efficiency of wind field in the future to make it more suitable for engineering application.

REFERENCES

[1] X. Fengjin and X. Ziniu, "Characteristics of tropical cyclones in China and their impacts analysis," *Natural Hazards*, vol. 54, no. 3, pp. 827–837, Mar. 2010, doi: 10.1007/s11069-010-9508-7.

[2] L. An, J. Wu, Z. Zhang, and R. Zhang, "Failure analysis of a lattice transmission tower collapse due to the super typhoon rammasun in july 2014 in hainan province, China," *J. Wind Eng. Ind. Aerodyn.*, vol. 182, pp. 295–307, Nov. 2018, doi: 10.1016/j.jweia.2018.10.005.

[3] L. An, Y. Guan, Z. Zhu, J. Wu, and R. Zhang, "Structural failure analysis of a river-crossing transmission line impacted by the super typhoon rammasun," *Eng. Failure Anal.*, vol. 104, pp. 911–931, Oct. 2019, doi: 10.1016/j.engfailanal.2019.06.069.

[4] X. Fu, H.-N. Li, and T.-H. Yi, "Research on motion of wind-driven rain and rain load acting on transmission tower," *J. Wind Eng. Ind. Aerodyn.*, vol. 139, pp. 27–36, Apr. 2015, doi: 10.1016/j.jweia.2015.01.008.

[5] X. Fu and H.-N. Li, "Dynamic analysis of transmission tower-line system subjected to wind and rain loads," *J. Wind Eng. Ind. Aerodyn.*, vol. 157, pp. 95–103, Oct. 2016, doi: 10.1016/j.jweia.2016.08.010.
[6] *Typhoon Road Map in 2018*. Accessed: Jan. 2019. [Online]. Available: http://www.hainanqx.cn
[7] G.-M. Ma, C.-R. Li, J. Jiang, J.-Y. Liang, Y.-T. Luo, and Y.-C. Cheng, "A passive optical fiber anemometer for wind speed measurement on high-voltage overhead transmission lines," *IEEE Trans. Instrum. Meas.*, vol. 61, no. 2, pp. 539–544, Feb. 2012, doi: 10.1109/TIM.2011.2164837.
[8] H. Geng, Y. Huang, S. Yu, J. Yu, H. Hou, and Z. Mao, "Research on early warning method of overhead transmission line damage caused by typhoon disaster," *Procedia Comput. Sci.*, vol. 130, pp. 1170–1175, 2018, doi: 10.1016/j.procs.2018.04.153.
[9] T. Hu, X. Wang, D. Zhang, G. Zheng, Y. Zhang, Y. Wu, and B. Xie, "Study on typhoon center monitoring based on HY-2 and FY-2 data," *IEEE Geosci. Remote Sens. Lett.*, vol. 14, no. 12, pp. 2350–2354, Dec. 2017, doi: 10.1109/LGRS.2017.2764620.
[10] V. Corcione, F. Nunziata, and M. Migliaccio, "Megi typhoon monitoring by x-band synthetic aperture radar measurements," *IEEE J. Ocean. Eng.*, vol. 43, no. 1, pp. 184–194, 2017, doi: 10.1109/JOE.2017.2700558.
[11] J. D. Hawkins, F. J. Turk, T. F. Lee, and K. Richardson, "Observations of tropical cyclones with the SSMIS," *IEEE Trans. Geosci. Remote Sens.*, vol. 46, no. 4, pp. 901–912, Apr. 2008.
[12] S. Lin, W. Fang, X. Wu, Y. Chen, and Z. Huang, "A spark-based high performance computational approach for simulating typhoon wind fields," *IEEE Access*, vol. 6, pp. 39072–39085, 2018, doi: 10.1109/ACCESS.2018.2850768.
[13] E. F. Thompson and V. J. Cardone, "Practical modeling of hurricane surface wind fields," *J. Waterway, Port, Coastal Ocean Eng.*, vol. 122, no. 4, pp. 195–205, 1996, doi: 10.1061/(ASCE)0733-950X(1996)122:4(195).
[14] P. N. Georgiou, A. G. Davenport, and B. J. Vickery, "Design wind speeds in regions dominated by tropical cyclones," *J. Wind Eng. Ind. Aerodyn.*, vol. 13, nos. 1–3, pp. 139–152, 1983, doi: 10.1016/0167-6105(83)90136-8.
[15] L. J. Shapiro, "The asymmetric boundary layer flow under a translating hurricane," *J. Atmos. Sci.*, vol. 40, no. 8, pp. 1984–1998, 1983, doi: 10.1175/1520-0469(1983)040<1984:TABLFU>2.0.CO;2.
[16] Y. Meng, M. Matsui, and K. Hibi, "An analytical model for simulation of the wind field in a typhoon boundary layer," *J. Wind Eng. Ind. Aerodyn.*, vol. 56, pp. 291–310, Dec. 1995, doi: 10.1016/0167-6105(94)00014-5.
[17] Y. Meng, M. Matsui, and K. Hibi, "A numerical study of the wind field in a typhoon boundary layer," *J. Wind Eng. Ind. Aerodyn.*, vols. 67–68, pp. 437–448, Dec. 1997, doi: 10.1016/s0167-6105(97)00092-5.
[18] G. J. Holland, "An analytic model of the wind and pressure profiles in hurricanes," *Monthly Weather Rev.*, vol. 108, no. 8, pp. 1212–1218, Aug. 1980, doi: 10.1175/1520-0493(1980)108<1212:AAMOTW>2.0.CO;2.
[19] M. P. Kleeman, B. A. Seibert, G. B. Lamont, K. M. Hopkinson, and S. R. Graham, "Solving multicommodity capacitated network design problems using multiobjective evolutionary algorithms," *IEEE Trans. Evol. Comput.*, vol. 16, no. 4, pp. 449–471, Aug. 2012, doi: 10.1109/TEVC.2011.2125968.
[20] V. Cavaliere, A. Formisano, R. Martone, and M. Primizia, "A genetic algorithm approach to the design of split coil magnets for MRI," *IEEE Trans. Appiled Supercond.*, vol. 10, no. 1, pp. 1376–1379, Mar. 2000, doi: 10.1109/77.828494.
[21] D. S. Zhang, "Wires mechanics calculation," in *Design Handbook of High Voltage Transmission Line for Power Engineering*, 2nd ed. Beijing, China: China Power Press, 2003, pp. 167–172.
[22] *The Key Parameters of Typhoon Rammasun*. Accessed: Dec. 2014. [Online]. Available: http://typhoon.weather.com.cn/
[23] M. Sobol', "Global sensitivity indices for nonlinear mathematical models and their Monte Carlo estimates," *Math. Comput. Simul.*, vol. 55, nos. 1–3, pp. 271–280, 2001, doi: 10.1016/S0378-4754(00)00270-6.

LIQIANG AN was born in Hebei, China, in 1974. He received the Ph.D. degree in thermal engineering from North China Electric Power University, in 2006. He is currently a Ph.D. Supervisor with North China Electric Power University. His main research interests include dynamic response analysis of transmission line under typhoon weather and transmission line health status intelligent perception technology.

YONGYU GUAN was born in Guangdong, China, in 1995. He received the bachelor's degree in mechanical engineering from North China Electric Power University, in 2018, where he is currently pursuing the master's degree. His primary research interests include flashover of transmission line and wind loads simulation of transmission line under typhoon weather.

ZHIJIAN ZHU was born in Zhejiang, China, in 1997. He received the bachelor's degree in mechanical engineering from North China Electric Power University, in 2018, where he is currently pursuing the master's degree. His research interests include the response of transmission towers and conductor galloping under typhoon weather.

JINGLI LIU is currently an Engineer of the State Grid Hebei Electric Power Company Ltd., Baoding Power Supply Branch Company. His research interests include fault diagnosis and maintenance of power equipment.

ZHUOBO NIU is currently an Engineer of the State Grid Hebei Electric Power Company Ltd., Baoding Power Supply Branch Company. His research interests include on-line monitoring of power equipment and maintenance of transmission lines.